

Effects of microplasma treatment on stratum corneum lipid molecule

メタデータ	言語: eng 出版者: 公開日: 2020-05-19 キーワード (Ja): キーワード (En): 作成者: Kristof, Jaroslav, Aoshima, T, Blajan, Marius, Shimizu, Kazuo メールアドレス: 所属:
URL	http://hdl.handle.net/10297/00027483

Effect of Microplasma Treatment on Stratum Corneum Lipid Molecule

J. Kristof¹, T. Aoshima², M. Blajan³ and K. Shimizu^{1,2,3}

¹Graduate School of Science and Technology, Department of Optoelectronics and Nanostructure Science, Shizuoka University, Johoku, Hamamatsu, Shizuoka 432 8561, Japan

²Graduate School of Engineering, Shizuoka University, Johoku, Hamamatsu, Shizuoka 432 8561, Japan

³Organization for Innovation and Social Collaboration, Shizuoka University, Johoku, Hamamatsu, Shizuoka 432 8561, Japan

E-mail: jaroslav.kristof@gmail.com, shimizu@cjr.shizuoka.ac.jp

The stratum corneum is a lipid matrix with embedded corneocytes, this layer protects body against foreign substances and the outer environment. However, the lipid matrix is permeable to selective molecules and this permeability can be improved by several methods. One of these methods includes microplasma irradiation of the skin. Stearic acid is a model fatty acid from the lipid matrix of stratum corneum. In this study, the interaction between microplasma and stearic acid was investigated. Plasma was generated at a low voltage of about 800 V ($0-V_{\text{peak}}$) using a thin dielectric ($\sim 30 \mu\text{m}$) as a barrier. The plasma electrode treated the lipids under an argon atmosphere at a frequency of 25 kHz. The results of the microplasma treatment were investigated by ATR-FTIR and XPS. The concentrations of C, O and N atoms were determined before and after the microplasma treatment. Also, functional groups of C-C/C-H, C-O, C=O, OH-C=O, N-C=O were identified in the carbon spectra. The structures of stearic acid were evaluated by analysis of CH₂, CH₃ and C=O bands in ATR-FTIR spectrum.

1. Introduction

The stratum corneum is the upper layer and the main barrier of the skin which protects the body against an outer environments. The stratum corneum consists of corneocyte cells situated in a lipid-rich matrix, this lipid matrix represents a route for drug delivery through the skin used in medical applications. Recently, plasma devices are been investigated as a skin permeability enhancers¹⁻⁸). The stratum corneum lipids in the lipid matrix are organized in a lamellar layers⁹). The lipid matrix composes of fatty acids (9%) with a small fraction of cholesterol sulfate (2%), cholesterol esters (10%), cholesterol (27%) and ceramides (41%)¹⁰). Among the fatty acids, the highest fraction represents saturated fatty acids such as stearic acid (10%), palmitic acid (10%), hexacosanoic acid (10%), behenic acid (15%), lignoceric acid (25%) and other unsaturated fatty acids represent a lower concentration¹¹). The saturated fatty acids are long straight molecules, so they can be very close to each other and have higher melting temperature; also, they are in a solid phase in the room temperature. This indicates that saturated fatty acids contribute to the barrier effect of the skin. On the other hand, unsaturated fatty acids do not always have straight shapes, they can be bent. This indicates that the space between them is larger. They have a very low melting temperature and can be in a liquid phase at the room temperature. These properties show that the presence of unsaturated fatty acids makes the skin more permeable. Plasma discharge is capable of creating many reactive particles. Investigation of interaction of the air plasma with the skin lipids was presented by Marchewski *et al.*¹²) and Hirschberg *et al.*¹³). These works showed that the plasma treated lipids increased the concentration of oxygen and nitrogen atoms in the samples, suggesting oxidation and nitration of the lipids or the lipids removal. Molecular dynamics simulation of OH and O radical reaction with α -linolenic acids (non-saturated fatty acid) demonstrated creation of double bonds, alcohols or aldehyde formation¹⁴). Molecular dynamics simulation realized in the lipid bilayer composed of cholesterol, ceramides and fatty acids showed also aldehydes formation and ceramide dissociation¹⁵). The barrier of the lipid bilayer is the most difficult to penetrate for H₂O₂ following HO₂ and OH, and almost no barrier exists against O₂ and similarly for NO¹⁶). Drug delivery through the skin using a plasma, instead of needles has some advantages; the lipid structures are used as the main route for drug delivery in the case of the plasma. So, it is necessary to investigate the changes of the skin lipids by the plasma treatment. We chose simple lipid to reduce problem of the complicated skin structure and to make it as simple as possible for analysis. Stearic acid was taken as a model lipid of the lipid membrane in the stratum corneum. The aim of this study is the investigation of argon microplasma interaction with the stearic acid using ATR-FTIR

and XPS. The composition and the structure of the stearic acid were analyzed.

2. Experimental methods

2.1 Experimental setup

A microplasma dielectric barrier discharge was generated by a thin-film electrode with a thickness of 200 μm and the electrodes were separated by a 30 μm thick dielectric. 18% of surface of the electrode composed of holes and plasma was generated at the surface closer to the grounded electrode which was facing the treated skin. Atmospheric argon microplasma was generated at a voltage of 800 V and a frequency of 25 kHz by a Neon transformer (ALPHA Neon M-5, LECIP)⁶⁾. The gas flow of was set at 5 L/min by a flow meter (Yamato) (Fig. 1).

2.2 Sample preparation

Stearic acid was in the form of a wax. The samples were set on an aluminum foil on a heater and heated to the temperature above the melting point until the samples changed to the liquid state. The liquid samples were placed on a cold metallic holder until the lipid solidified. The samples were round in its shape with a diameter approximately 5 mm. Prepared samples were treated by the argon microplasma discharge for 5 minutes at the distance of 0.5 – 1 mm from the surface of the electrode. The prepared samples were investigated by XPS and ATR-FTIR spectroscopy before and after the plasma treatment.

2.3 XPS analysis

X-ray photoelectron spectroscopy (XPS) is an effective method for analyzing the elements of the solid surface layer from 0.5 to 5 nm. X-ray photoelectron spectra of the stearic acid were obtained with Shimadzu ESCA 3400 instrument equipped with a monochromatic Mg $K\alpha$ X-ray source (1150 eV). The concentrations of the elements were determined by carbon C 1s, oxygen O 1s and nitrogen N 1s peaks of the XPS spectra.

2.4 ATR-FTIR analysis

Attenuated Total Reflectance-Fourier Transform InfraRed (ATR-FTIR) spectrometer (Jasco FT/IR 6300 with ATR PRO610P-S) with a diamond prism was used to observe the stearic acid. Accumulatively, 150 scans of spectra were recorded at a resolution of 8 cm^{-1} .

The peaks in the spectra were fitted by Gaussian function. To increase the precision, also 4th derivative was fitted at the same time.

3. Results and discussion

3.1 Microplasma treatment of Stearic acid

Stearic acid is a saturated carboxylic acid present in stratum corneum, it composes of 18 carbon atoms, 36 hydrogen atoms and 2 oxygen atoms respectively ($C_{18}H_{36}O_2$). Its melting temperature ranges from 69 – 71 °C and a boiling temperature is 361°C.

3.2 X-ray photoelectron spectroscopy of Stearic acid¹⁷⁾

Excluding hydrogen atoms, stearic acid has a chemical composition of 10% oxygen and 90% carbon. The elemental compositions were resolved by the XPS measurement: $9.4\% \pm 1.7\%$ of oxygen and $90.6 \pm 2\%$ of carbon. Simultaneously, the microplasma treated stearic acid was oxidized and nitrated. The concentration of oxygen enlarged to $12.7\% \pm 1.7\%$ and that of nitrogen, from 0% to $1\% \pm 0.3\%$. XPS spectra of the carbon were normalized to the area under the peak (after subtraction of the background). In the case of the Ar microplasma treated stearic acid, the carbon spectra in (Fig. 2A, B) was able to fit with five peaks of (C-C/C-H, C-O, C=O, O=C-N, O=C-OH) and in the case of non-treated stearic acid, only by four peaks of (C-C/C-H, C-O, C=O, O=C-OH).

The O=C-OH group and hydrocarbon chain should be the only composition of the non-treated samples, nevertheless, C=O functional group of ketones was observed in XPS spectrum. This implies that some impurities were present in the stearic acid sample. Before the measurements, the sample was melted by heating to approximately 90°C. However, generating ketones (the hydrocarbons only with C=O group) requires the temperature above 200°C and requires the presence of catalysts¹⁸⁾. Fig. 2C shows the areas of the functional groups of the carbon spectra normalized to whole carbon area of the sample. The microplasma treatment resulted in a decrease in number of C-C/C-H and increased in number of C-O, C=O functional groups including the groups with incorporated nitrogen.

In the microplasma treated sample, nitrogen presence was confirmed in the carbon spectra by O=C-N at the position of 288.5 eV and also the nitrogen peak was spotted at the position of 400.5 eV with FWHM of 1.75 eV. The typical position of C-N and O=C-N peaks is between 399 – 401.1 eV and 399.8 – 400.9 eV, respectively¹⁹⁾.

Bernadelli *et al.*²⁰⁾ investigated DC discharge plasma treatment of the stearic acid using Ar gas in the mixtures of Ar+10%O₂ and Ar+10%H₂, their study revealed that the surface was favorably etched in the discharge zone and grafted in the post-discharge zone (the zone without electrons, charged particles and chemically active species). The etching happened to

be most effective in mixture of Ar+10%O₂ due to chemical sputtering but was less effective in Ar and Ar+10%H₂ discharges. Carboxylic group (-COOH) was removed at a low temperature (about 45°C) before breaking of C-C/C-H and the functionalization process started at the higher temperatures (~60°C). Volatile products production such as alcohols, ketones, acids or esters, during discharge treatment was noticed in the Ar+10%O₂ mixture²¹). The etching of stearic acid within the confines of the post-discharge zone occurred by atomic oxygen through the breakdown of C-C bonds²²). The functionalization was done by the grafting OH group to the hydrocarbon chain and C=O could be formed after the longer treatment by the oxidation of grafted OH. The investigation of the products generated after the plasma treatment revealed the presence of carboxylic acids with shorter chains²²). Noel *et al.*²³) surveyed on the treatment of stearic acid in the microwave Ar-N₂ and Ar-O₂ atmospheric post-discharge, their results also confirmed that there was a higher etching rate by Ar-O₂ mixture than Ar-N₂ and also the formation the shorter chain carboxylic acids. On the other hand, in the Ar-N₂ post-discharge, higher amount of C=C bonds were produced. By mass spectrometry, nitrogen presence was confirmed in both discharges but only via observation of the short chain ions such as CN, HCN, NH etc. Moreover, studies on the exposure of a polyethylene film to the oxygen radicals or the oxygen plasma revealed only minor difference between them in the production of C=O, COOH and OH. This implied that the oxygen radicals were in charge for the creation of these functional groups²⁴). The nitrogen functional groups investigation was not revealed in details but the creation of amide and amine groups were observed in the polyethylene films after nitrogen plasma treatment²⁵).

3.3. FTIR spectroscopy of Stearic acid

3.3.1 Methylene CH₂ rocking band (717 cm⁻¹ – 730 cm⁻¹)¹⁷⁾

The lateral packing structure of hydrocarbon chains can be characterized by methylene rocking vibration at 720 cm⁻¹. Splitting of CH₂ rocking peak into two bands near 720 cm⁻¹ and 730 cm⁻¹ can be characterized as Orthorhombic packing. Increase in temperature can change the orthorhombic structure to the liquid hexagonal packing. In the course of this process, the band at 730 cm⁻¹ is approaches to 720 cm⁻¹ and finally disappears. The expansion of the lattice and the loosening of the structure can be explained by this phenomenon; however, heating is not the only method to change the lipid structure. Zhang *et al.*²⁶) proved that the presence of an impurities could increase the lattice dimension. In their study, they compared the polyethylene lattice with a halogen impurity, as the number of the impurities increased, the distance between the above-mentioned split bands decreased. When the peak

is near 717 cm^{-1} , it would be an evidence of a triclinic organization; the peak intensity increases in the direction from the liquid organization through the hexagonal and orthorhombic to the triclinic²⁷). The intensity ratio can designate the crystallinity²⁸). Doublet is usually visible for less than 40°C .

In our studies, the spectra of non-treated stearic acid were clearly composed of two peaks; the second peak came into sight at 728.5 cm^{-1} . This band moved to the lower wavenumbers to the 726.9 cm^{-1} after the plasma treatment of stearic acid, indicating an increase in the lattice dimensions. The ratio of absorbencies (A_{730}/A_{720}) was changed from 0.76 to 1.75.

3.3.2 Progression bands ($1185\text{ cm}^{-1} - 1350\text{ cm}^{-1}$)

The presence of the orthorhombic packaging was also confirmed by the progression bands (from 1185 cm^{-1} to 1350 cm^{-1}). The progression bands come from wagging of the CH_2 bands and the position depends on the “trans” or “cis” conformation of stearic acid. When alkyl chains are disordered, wagging decreases and peaks are replaced by other bands present in different conformation of alkyl chain^{29, 30}). The number of the progression bands is $N/2$, where the N is the number of CH_2 bands.

Our observation showed that the progression bands were still present in stearic acid sample before and after the plasma treatment and there was no difference in their positions. However, the intensities of the progression bands decreased after the exposure to the microplasma. This observation suggests a disorder in the orthorhombic structure of stearic acid after the microplasma treatment.

3.3.3 CH_2 Scissoring band ($1450\text{ cm}^{-1} - 1485\text{ cm}^{-1}$)

Another band characterizing the lipid structure is scissoring CH_2 split band at 1463 cm^{-1} and 1472 cm^{-1} . The bands are approaching during changing of the structure of molecules and finally, only one band at 1464 cm^{-1} is present in the hexagonal and liquid packing.

Distance 9 cm^{-1} of the scissoring band decrease to 6.7 cm^{-1} after the microplasma treatment of stearic acid. The measurement suggests that there was some disorder in the orthorhombic structure of steric acid caused by the microplasma treatment¹⁷).

3.3.4 $\text{C}=\text{O}$ stretching band ($1650\text{ cm}^{-1} - 1750\text{ cm}^{-1}$)

This area is sensitive to hydrogen bonding, $\text{C}=\text{O}$ stretching band of non-treated and plasma treated sample was composed of several peaks (Fig. 3B, C). Han *et al.*³¹) deconvoluted $\text{C}=\text{O}$ band of stearic acid into 4 peaks at 1760 cm^{-1} (monomer), 1715 cm^{-1} (*open loop*-dimer or

catamer), 1703 cm^{-1} (*cis*-dimer) and 1685 cm^{-1} (*trans*-dimer). We were able to identify 7 peaks at wavenumbers 1664 cm^{-1} (A), 1677 cm^{-1} (B), 1688 cm^{-1} (C), 1701 cm^{-1} (D), 1712 cm^{-1} (E), 1725 cm^{-1} (F), 1742 cm^{-1} (G). The peaks B, C, D could be identified as *trans*-, *cis*- and *open loop*- dimers of stearic acid. The C=O stretching band was composed of 76% (before the microplasma treatment) and 70% (after the microplasma treatment) of the B, C, D peaks. Other peaks can belong to stearic acid with different interactions with hydrogen bonding. The peaks at higher wavenumbers were characteristic for the weaker hydrogen bonding. The absorbance of the peaks at higher wavenumbers is higher in the plasma treated sample than in the non-treated sample. This observation implies that the microplasma treatment was weakening the hydrogen bonding.

3.3. Methylene and methyl CH_2 stretching band (2800 cm^{-1} – 3000 cm^{-1})

The conformation of the hydrocarbon chain could be characterized by the CH_2 symmetric stretching band. This band was moved from 2846.7 cm^{-1} to 2848.1 cm^{-1} after the microplasma treatment. These values indicated changes in orthorhombic packing. Lipids are composed of long hydrocarbon chains. The lipid tail consists of the CH_2 groups with the CH_3 group at the end of the chain. As the number of the CH_3 functional groups is proportional to the absorbance of the symmetric stretches of the CH_3 . The number of the CH_2 functional groups is proportional to the absorbance of the symmetric stretches of the CH_2 . The ratio of these bands can characterize the length of the lipid chains. When this ratio changes, the length of the hydrocarbon chain is also changed. Another explanation of the decrease the CH_2 stretching band can be oxidation. Average ratio of the absorbances of CH_2/CH_3 stretching band decreased from 2.37 to 1.57 that means that number of CH_2 functional groups was decreased by breaking of the bond or by the oxidation. During the microplasma treatment, it decreased about 34%.

All these results indicated the structural changes in the orthorhombic packing, the disorder and the increase of the lattice dimension, the oxidation/chain breaking after the microplasma treatment of stearic acid. These changes can affect the organization of lipids in the lipid membranes after the plasma treatment³²⁾

4. Conclusions

Argon microplasma interaction with the lipid such as stearic acid was investigated. The results of the plasma treated and the non-treated samples were compared by ATR-FTIR and XPS analysis. The plasma treatment of stearic acid caused nitration and oxidation of the

molecule at the same time. Oxidation could cause change of the structure, and the increase of the dimension of the lattice of stearic acid. This was indicated by observation of the methylene CH₂ rocking band (approaching of two bands – increase of the lattice), the progression bands (decreasing of absorbance – change of the structure), the CH₂ scissoring band (approaching of two bands – change of the structure), and the symmetric methylene CH₂ stretching band (shift of the band – change of the structure, disorder). The ratio of the CH₂ and CH₃ stretching bands showed decrease of the amount of CH₂ functional groups. The C=O stretching vibrational band showed the increase of structures with the weaker hydrogen bonding and the decrease of the structures with the stronger hydrogen bonding. As the plasma can affect the structure of lipids, this can change the fluidity of the lipid membranes and their organization and also play a role in microplasma drug delivery.

References

- 1) S. Kalghatgi, C. Tsai, R. Gray, D. Pappas, 22nd Int'l Symposium on Plasma Chemistry, 2015, p. O-22-6.
- 2) K. Shimizu, A. N. Tran, J. Kristof, M. Blajan, Proceedings of the 2016 Electrostatics Joint Conference, 2016, p. I4.
- 3) J.-H. Choi, S.-H. Nam, Y.-S. Song, H.-W. Lee, H.-J. Lee, K. Song, J.-W. Hong, G.-Ch. Kim, Arch. Dermatol. Res. **306**(7), 635 (2014).
- 4) H. Y. Lee, J. H. Choi, J. W. Hong, G. Ch. Kim, H. J. Lee, J. Phys. D: Appl. Phys. **51**, 215401 (2018).
- 5) M. Gelker, Ch. C. Müller-Goymann, W. Viöl, Clinical Plasma Medicine **9**, 34 (2018).
- 6) J. Kristof, H. Miyamoto, A. N. Tran, M. Blajan, and K. Shimizu, Biointerphases **12**(2), 02B40 (2017).
- 7) K. Shimizu, An. N. Tran, K. Hayashida, M. Blajan, J. Phys. D: Applied Physics **49**(31), 315201 (2016).
 - 8) K. Shimizu, Plasma Medicine **5**(2-4), 205 (2016).
 - 9) J. R. Hill, P. W. Werz, Biochimica et Biophysica Acta **1616**, 121 (2003).
 - 10) T. M. Suhonen, J. A. Bouwstra, A. Urti, Journal of Controlled Release **59**, 149 (1999).
 - 11) T.-K. Lin, L. Zhong, J. L. Santiago, Int. J. Mol. Sci. **19**, 70 (2018).
 - 12) M. Marschewski, J. Hirschberg, T. Omairi, W. Viol, S. Emmert, W. Maus-Friedrichs, Exp. Dermatol. **21**, 921 (2012).
 - 13) J. Hirschberg, L. Loewenthal, A. Krupp, S. Emmert, W. Viöl, Natural Science **8**, 125

- (2016).
- 14) J. Van der Paal, S. Aernouts, A. C. T. van Duin, E. C. Neyts and A. Bogaerts, *J. Phys. D: Appl. Phys.* **46**, 395201 (2013).
 - 15) J. Van der Paal, C. C. Verlaack, M. Yusupov, E. C. Neyts, A. Bogaerts, *J. Phys. D: Appl. Phys.* **48**, 155202 (2015).
 - 16) J. Van der Paal, C. Verheyen, E. C. Neyts, A. Bogaerts, *Sci Rep.* **7**, 39526, (2017).
 - 17) J. Kristof (2018), *Study of atmospheric plasma interaction to enhance permeability*. Shizuoka University, Hamamatsu, Japan.
 - 18) S.A.W. Hollak, J.H. Bitter, J. van Haveren, K.P. de Jong, D. S. van Es, *RSC Adv.* **2**, 9387 (2012).
 - 19) J. S. Stevens, S. L. M. Schroeder, *Encyclopedia of Physical Organic Chemistry* (Wiley, New Jersey, 2017) p. 3241.
 - 20) E. A. Bernardelli, M. Mafra, A. M. Maliska, T. Belmonte, A. N. Klein, *Materials Research* **16**(2): 385-391 (2013).
 - 21) E. A. Bernardelli, T Souza, M. Mafra, A. M. Maliska, T. Belmonte, A. N. Klein, *Materials Research* **14**(4), 519 (2011).
 - 22) E. A. Bernardelli, T. Belmonte, D. Duday, G. Frache, F. Pncin-Epaillard, C. Noel, P. Choquet, H.-N. Migeon, A. M. Maliska, *Plasma Chem Plasma Process* **31**, 189 (2011).
 - 23) C. Noel, D. Duday, S. Verdier, P. Choquet, T. Belmonte, H.-N. Migeon, *Plasma Process. Polym.* **6**, S187 (2009).
 - 24) N. Inagaki, K. Yamamoto, *Nippon Kagaku Kaishi* **1987**, 2031 (1987).
 - 25) N. Inagaki, *Plasma Surface Modification and Plasma Polymerization* (Technomic publishing company, Lancaster, 1996), p. 32.
 - 26) X. Zhang, L. Santonja-Blasco, K. B. Wagener, E. Boz, M. Tasaki, K. Tashiro, R. G. Alamo, *J. Phys. Chem. B* **121** (43), 10166 (2017).
 - 27) B. Xie, G Liu, S. Jiang, Y. Zhao, D. Wang, *J. Phys. Chem. B* **112** (42), 13310 (2008).
 - 28) M. B. Sajwan, S. Aggarwal, R.B. Singh, *The Indian Journal of Criminology & Criminalistics* **XXIX** (1), 55 (2008).
 - 29) S. Zhu, M. Heppenstall-Butler, M. F. Butler, P. D. A. Pudney, D. Ferdinando, K. J. Mutch, *J. Phys. Chem. B* **109**(23), 11753 (2005).
 - 30) P. Garidel, A. Blume, W. Hubner, *Biochimica et Biophysica Acta* **1466**, 245 (2000).
 - 31) W.-R. Han, S.-B. Liu, Z.-G. Zhou; Y.-F. Chang, R.-S. Hu, H.-W. Yu, *PTCA (Part B: Chemical Analysis)* **50**, 11 (2014).

- 32) K. Shimizu, J. Kristof, M. G. Blajan, *Atmospheric Pressure Plasma - from Diagnostics to Applications*, (IntechOpen, London, 2019), p. 466

Figure Captions

Fig. 1. The microplasma electrode and the sample treatment by Ar gas. View from the bottom (left) side and the cross section (right).

Fig. 2. A: The carbon spectra of the non-treated stearic acid (grey solid line) and the microplasma treated stearic acid (solid black line). B: The carbon spectra of the non-treated stearic acid (black solid line), the microplasma treated stearic acid (black dashed line) and the fitted peaks (grey solid lines). C: The percentage of the functional groups in the non-treated, the microplasma treated sample normalized to the carbon peak area.

Fig. 3. A: FTIR spectrum of the non-treated stearic acid. B: The C=O stretching band composed of 7 peaks. FTIR spectrum of the 5 minutes Ar microplasma treated (grey solid line) and the non-treated stearic acid (black solid line). C: 4th derivative of the C=O stretching band. Maximums determine the position of the peaks.

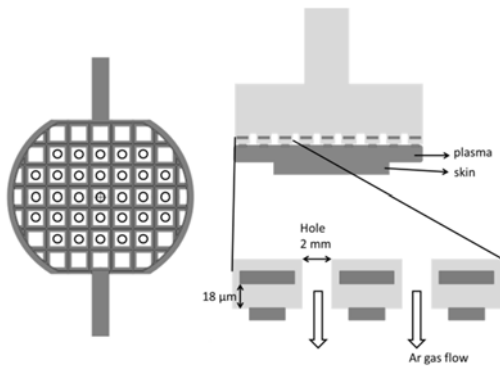


Fig. 1.

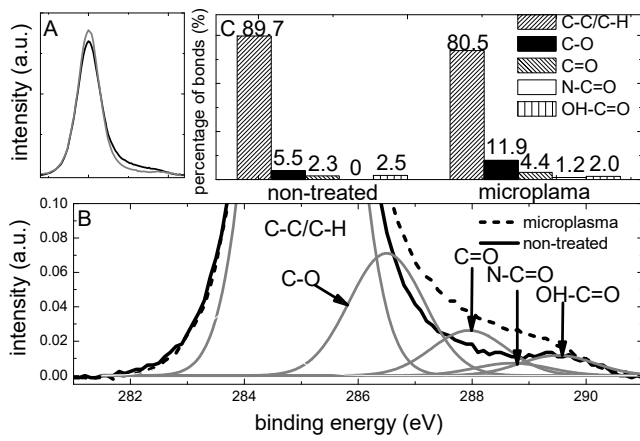


Fig. 2.

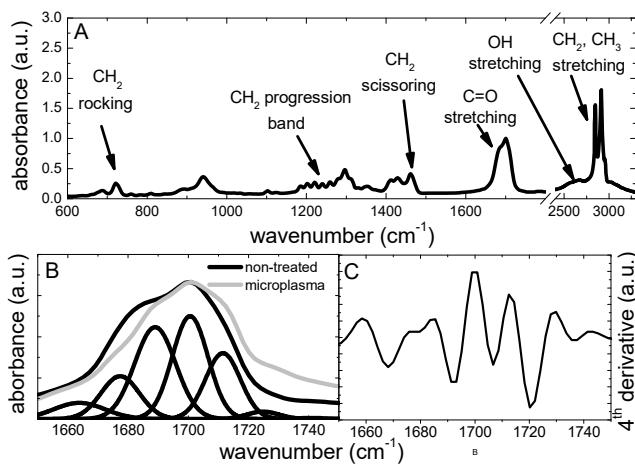


Fig. 3.